Supplementary Information (SI) for Journal of Materials Chemistry C.
This journal is © The Royal Society of Chemistry 2026

Ultrahigh electromechanical output in ferroelectric polymer via a continuous and aligned pore design

Linjie Zhu ,[a] Xiaofei Liu ,[a] and Xin Zhang*[a]

[a] School of Materials and Microelectronics & Center of Smart Materials and Devices, State Key Laboratory of Advanced Technology for Materials Synthesis and Processing, Wuhan University of Technology, Wuhan 430070, China.

*Corresponding author

E-mail: zhang-xin@whut.edu.cn

Steps and parameters of finite element analysis

Finite element analysis was performed to investigate the electromechanical response and internal electric field distribution of the CAP structure. A representative volume element was constructed to model the microstructure, consisting of a cuboid domain with embedded aligned pore channels. The surface charge density on the inner pore walls was calculated out of approximately 5.9 $\mu C \cdot m^{-2}$. Opposite charges were assigned to the upper and lower surfaces of the pores to represent the charge separation induced during charging. The dielectric constant of the P(VDF-TrFE) matrix was set to 12, while that of air inside the pores was taken as 1. The mechanical and electromechanical behavior of the system was described in Voigt notation, with the compliance matrix and electromechanical coupling matrix are derived as follows, the compliance matrix of P(VDF-TrFE) is:

$$\begin{bmatrix} 0.40 & -0.14 & -0.27 & 0 & 0 & 0 \\ -0.14 & 0.40 & -0.27 & 0 & 0 & 0 \\ -0.27 & -0.27 & 0.67 & 0 & 0 & 0 \\ 0 & 0 & 0 & 1.85 & 0 & 0 \\ 0 & 0 & 0 & 0 & 1.85 & 0 \\ 0 & 0 & 0 & 0 & 0 & 1.08 \end{bmatrix} \times 10^{-9}\, Pa^{-1},$$

and the compliance matrix of air is:

$$\begin{bmatrix} 7 & 0 & 0 & 0 & 0 & 0 \\ 0 & 7 & 0 & 0 & 0 & 0 \\ 0 & 0 & 7 & 0 & 0 & 0 \\ 0 & 0 & 0 & 14 & 0 & 0 \\ 0 & 0 & 0 & 0 & 14 & 0 \\ 0 & 0 & 0 & 0 & 0 & 14 \end{bmatrix} \times 10^{-6}\, Pa^{-1},$$

and the electromechanical coupling matrix of P(VDF-TrFE) is:

$$\begin{bmatrix} 0 & 0 & 0 & 0 & 0 & 0 \\ 0 & 0 & 0 & 0 & 0 & 0 \\ 9.05 & 0.98 & -22.0 & 0 & 0 & 0 \end{bmatrix} \times 10^{-12}\, C \cdot N^{-1},$$

and air is all 0 since it has none piezoelectricity. The simulation was conducted under steady-state conditions. For the boundary conditions, a compressive stress of 50 kPa was applied uniformly on the top surface along the out-of-plane (z) direction. The bottom surface was mechanically fixed and electrically grounded, while the remaining boundaries were treated with default conditions.

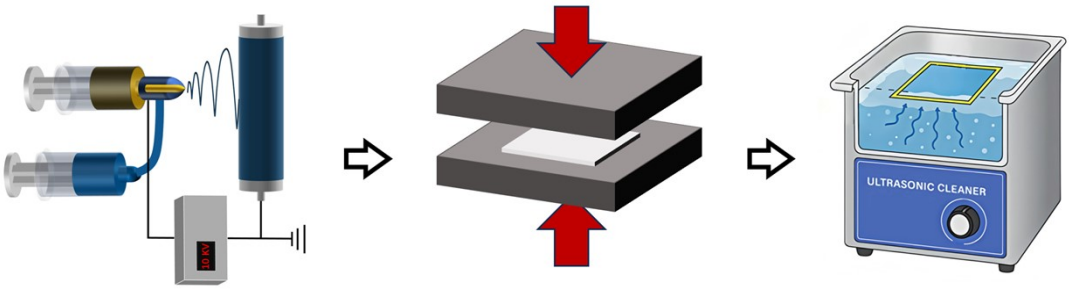

Figure S1. Schematic illustration of the fabrication process for CAP-structured P(VDF-TrFE) film.

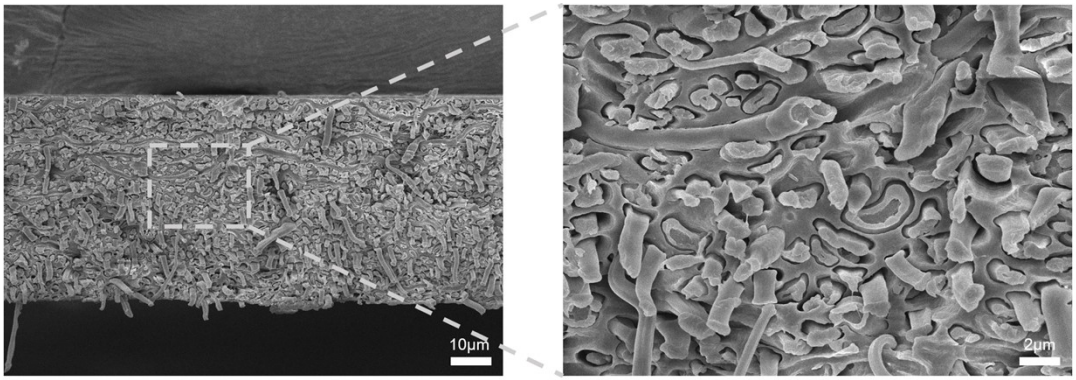

Figure S2. Cross-sectional SEM images of the CAP-structured P(VDF-TrFE) film before removal of PEI sacrificial template.

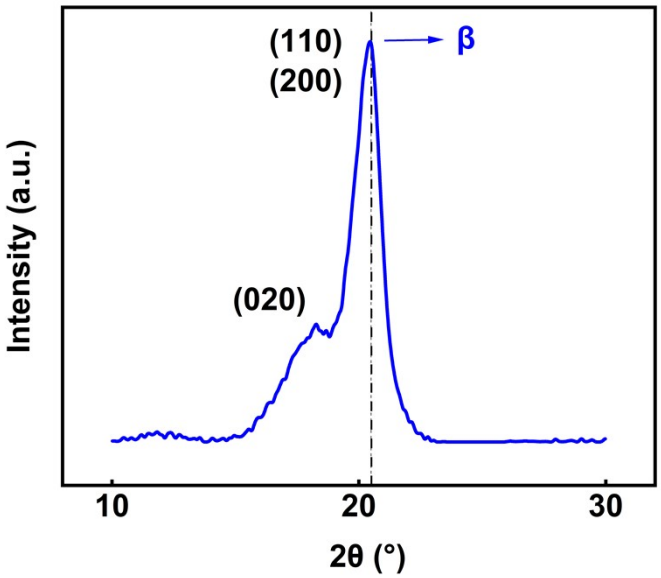

Figure S3. XRD patterns of the CAP-structured P(VDF-TrFE) film.

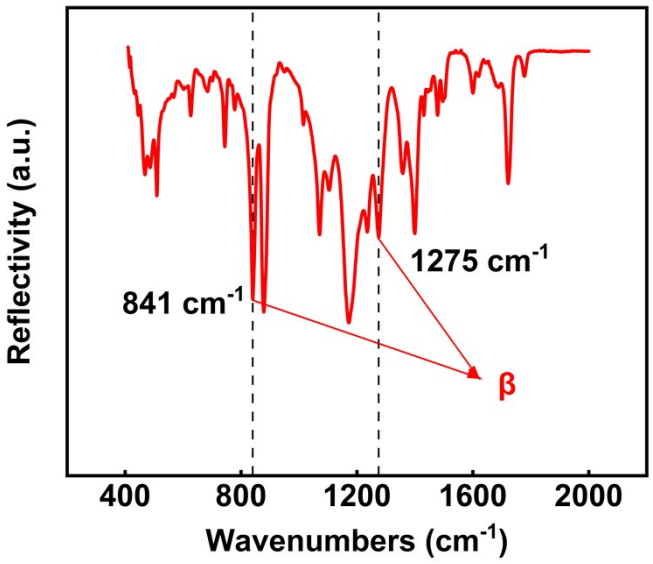

Figure S4. Fourier transform infrared (FTIR) spectra of the CAP-structured P(VDF-TrFE) film.

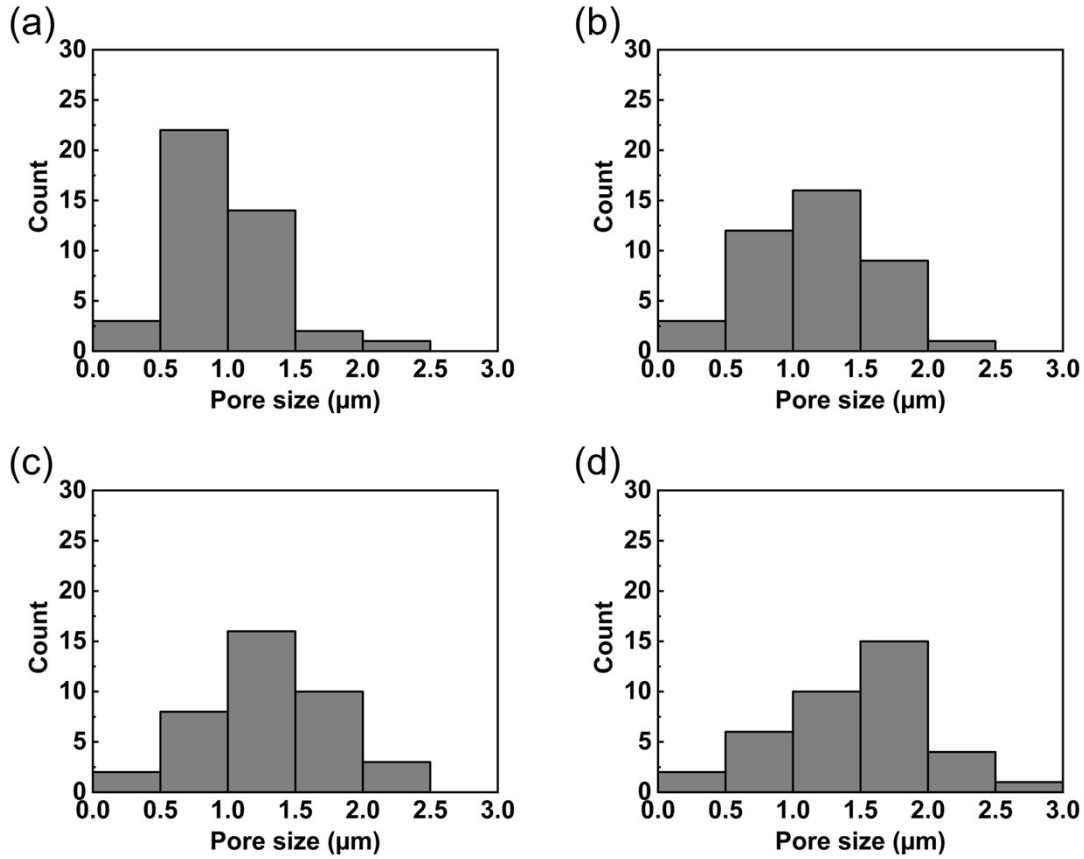

Figure S5. Pore sizes in CAP-structured P(VDF-TrFE) prepared with varying flow rates of PEI solutions during coaxial electrospinning: (a) 0.33 mL·h^{-1} with an average pore size of 0.94 μm, (b) 0.67 mL·h^{-1} with an average pore size of 1.10 μm, (c) 1.00 mL·h^{-1} with an average pore size of 1.22 μm, (d) 1.33 mL·h^{-1} with an average pore size of 1.41 μm.

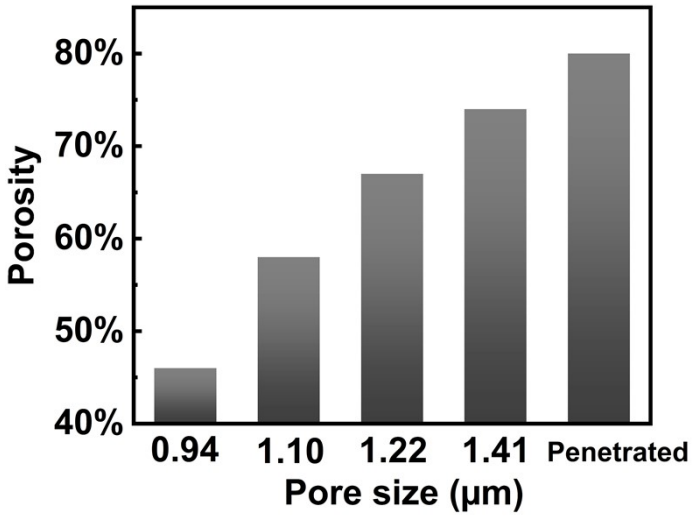

Figure S6. Quantitative correlation of porosity and pore size in CAP-structured P(VDF-TrFE) film.

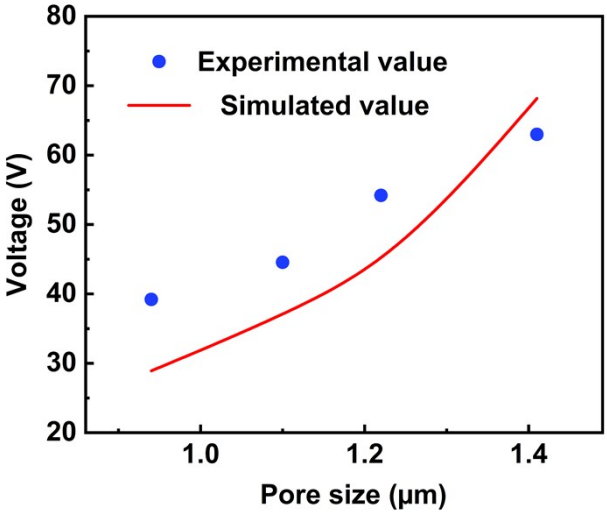

Figure S7. Comparison of experimental and simulated output voltage results for CAP-structured P(VDF-TrFE) films with varying pore sizes.

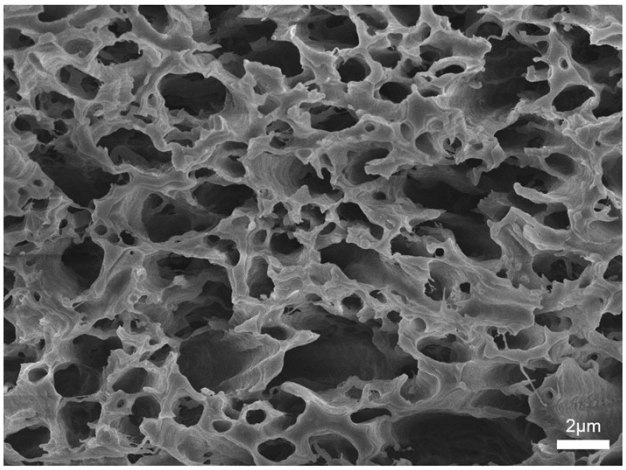

Figure S8. Cross-sectional SEM images of the PVDF-TrFE film with 3D continuous network pores.

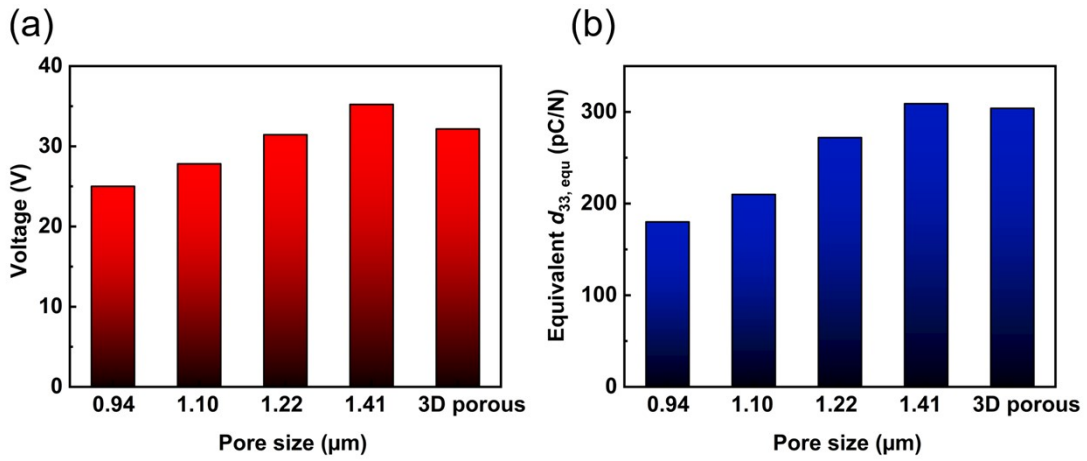

Figure S9. (a) Voltage and (b) equivalent piezoelectric coefficient $d_{33, equ}$ of uncharged CAP-structured P(VDF-TrFE) films with different pore sizes.

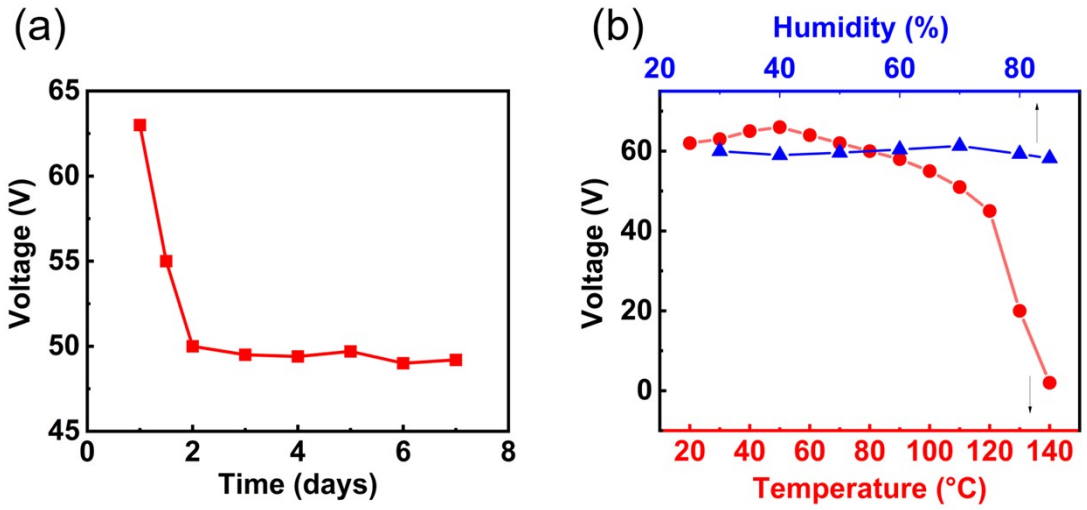

Figure S10. (a) Voltage of the film over 7 days. (b) Voltage of the film under temperature range from 20 to 140 ℃ and humidity range from 30% to 85%.

Table S1 The equivalent $d_{33,\,equ}$ of previously published piezoelectret materials and the CAP-structured P(VDF-TrFE) piezoelectret material in this work.

Material	Equivalent $d_{33,\,equ}$ ($pC \cdot N^{-1}$)	References
Multilayered COC	~1000	1
Multilayered PDMS	350	2
Multilayered FEP	5400	3
Multilayered PP	>3000	4
Multilayered FEP/Ecoflex/FEP	4050	5
Multilayered FEP/ePTFE/FEP/ePTFE/FEP	200	6
3D-printed ABS	~100	7
3D-printed P(VDF-TrFE)	1200	8
Foamed IXPP	650	9
Cellular PP	~200	10
CAP-structured P(VDF-TrFE)	5727	This work

References

1 Y. Li and C. Zeng, *Macromol. Chem. Phys.*, 2013, 214, 2733–2738.

2 A. Kachroudi, S. Basrour, L. Rufer, A. Sylvestre and F. Jomni, *Smart Materials and Structures*, 2016, 25, 105027.

3 L. Han, W. Zeng, Y. Dong, X. Wang and L. Lin, *Advanced Electronic Materials*, 2022, 8, 2200012.

4 Z. Ruan, Q. Hu, M. Zhang, W. Liu, G. Zhu, M. Chen and X. Zhang, *Appl. Phys. Lett.*, 2023, 122.

5 J. Zhong, Y. Ma, Y. Song, Q. Zhong, Y. Chu, I. Karakurt, D. B. Bogy and L. Lin, *ACS Nano*, 2019, 13, 7107–7116.

6 N. Wang, M. A. Baferani, R. Daniels, C. Wu, J. Huo, J. van Turnhout, G. A. Sotzing, R. Gerhard and Y. Cao, *Journal of Physics D: Applied Physics*, 2024, 57, 145502.

7 Y. A. O. Assagra, R. A. P. Altafim, R. A. C. Altafim and J. P. Carmo, *Electron. Lett*, 2015, 51, 2028–2030.

8 A. Kumar, D. Saini and D. Mandal, *Appl. Phys. Lett.*, 2022, 120.

9 X. Zhang, L. Wu and G. M. Sessler, *AIP Advances*, 2015, 5.

10 N. Wu, X. Cheng, Q. Zhong, J. Zhong, W. Li, B. Wang, B. Hu and J. Zhou, *Adv. Funct. Mater.*, 2015, 25, 4788–4794.